Integer Aperture Estimation

A Framework for GNSS Ambiguity Acceptance Testing

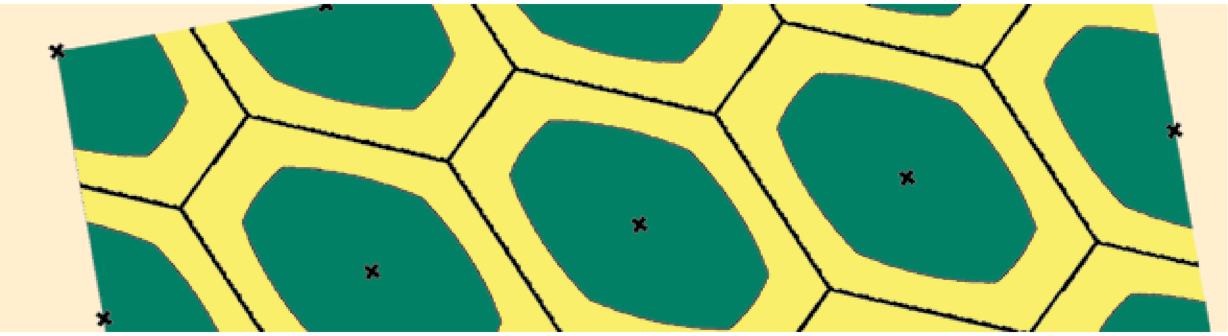

Tracking the carrier phase of GNSS signals has evolved into a widespread practice for achieving rapid and very accurate positioning. A key to this process is implementing a robust method for determining the number of carrier waves between a GNSS satellite and receiver, including any fractional wavelength, in a given signal transmission – so-called integer ambiguity resolution. Researchers have developed a variety of approaches for calculating the number of integers, but reliable means for testing and accepting the results of such calculations – a crucial factor for ensuring the integrity of such measurements – are not as well developed. This column introduces the principle of integer aperturte estimation and show how it can accomplish this goal.

PETER J. G. TEUNISSEN
CURTIN UNIVERSITY OF TECHNOLOGY, AND DELFT UNIVERSITY OF TECHNOLOGY
SANDRA VERHAGEN
DELFT UNIVERSITY OF TECHNOLOGY

Integer carrier-phase ambiguity resolution is the key to fast and high-precision GNSS positioning and navigation. It is the process of resolving the unknown cycle ambiguities of the carrier-phase data as integers. Once this has been done successfully, the very precise carrier-phase data will act as pseudorange data, thus making very precise positioning and navigation possible.

Procedures for carrier-phase ambiguity resolution not only consist of integer ambiguity estimation, but usually also include ambiguity acceptance testing. Such testing is important, in particular in light of the ever increasing integrity demands on GNSS solutions.

Although the statistical theory of integer ambiguity estimation is reasonably well established, this cannot yet be said of ambiguity acceptance testing. The aim of this article, therefore, is to present a unifying theoretical framework for ambiguity estimation and testing. It provides the tools for comparing and evaluating current procedures for acceptance testing and creates the possibility to devise new tests that are better than existing ones.

We will begin with a review of the four-step procedure for integer ambiguity resolution, including acceptance testing. Next, we will introduce the principle of integer aperture (IA) estimation and explain how and why this estimation principle provides us the framework we are looking for.

The following section will describe how we can evaluate the quality of IA estimation. Finally, we will discuss the way in which to define optimal IA estimators. Two such optimal IA estimators are presented, the *fail-rate constrained maximum success-rate estimator* and the *minimum mean penalty estimator*.

The Four Steps of Ambiguity Resolution

To describe the process for resolving carrier-phase ambiguities, we start with the mixed integer linear(ized) GNSS model,

$$E(y) = Aa + Bb,\ D(y) = Q_{yy},\ a \in \mathbb{Z}^n,\ b \in \mathbb{R}^p \qquad (1)$$

where *E(.)* and *D(.)* denote expectation and dispersion, respectively, and where the m-vector y contains the "observed minus computed," single-, dual- or multi-frequency carrier-phase and pseudorange (code) observables. The n-vector a contains the integer double-differenced (DD) ambiguities, and the real-valued p-vector b contains the remaining unknown parameters, such as baseline components (coordinates), atmospheric delay parameters (troposphere, ionosphere), and possibly (receiver, satellite) clock parameters and instrumental delays. Note that the parameterization in DD ambiguities does not require y to be in DD form.

Thus, y may be in undifferenced or single-differenced form as well. The $m \times (n+p)$ matrix (A,B) contains the given design matrices of a and b, respectively, and the $m \times m$ positive definite matrix Q_{yy} is the variance matrix of y.

The process of solving the GNSS model is usually divided into the following four steps (**Figure 1**).

1. Float Solution. In the first step, the integer nature of the ambiguities is discarded and a standard least-squares (LS) parameter estimation is performed. As a result, one obtains the so-called float solution, together with its variance-covariance matrix,

$$\begin{bmatrix} \hat{a} \\ \hat{b} \end{bmatrix}, \begin{bmatrix} Q_{\hat{a}\hat{a}} & Q_{\hat{a}\hat{b}} \\ Q_{\hat{b}\hat{a}} & Q_{\hat{b}\hat{b}} \end{bmatrix} \tag{2}$$

Other forms than batch least-squares — such as, for example, recursive LS or Kalman filtering — may, of course, also be used to come up with a float solution. Such choices will depend on the application and on the structure of the GNSS model.

2. Integer solution: In the second step, the real-valued float ambiguity solution $\hat{a}$ is further mapped to an integer solution

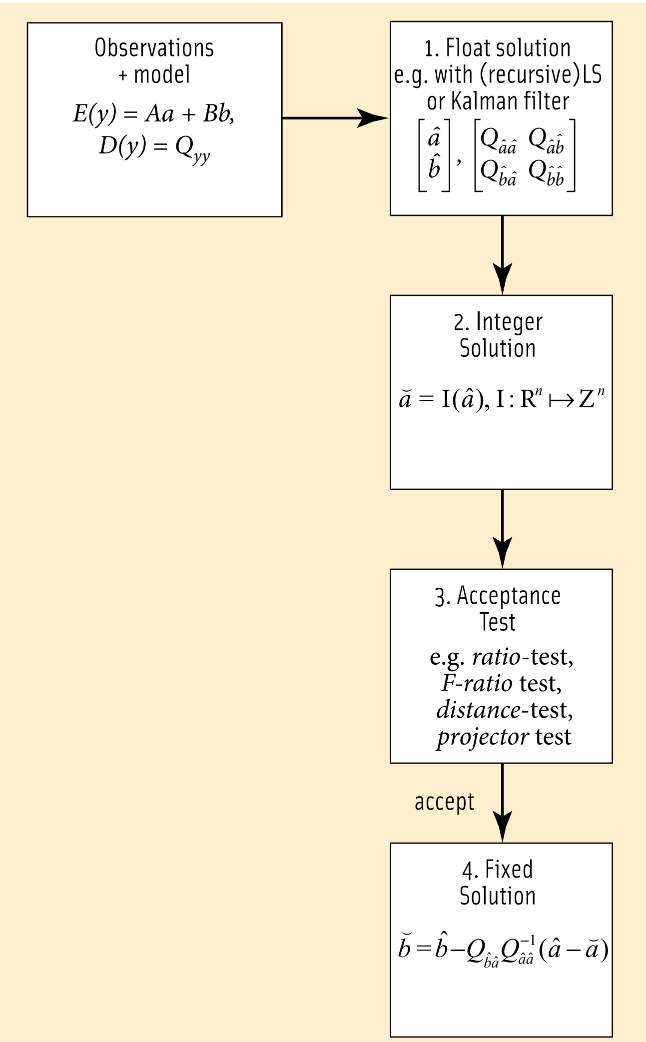

FIGURE 1 The four steps of GNSS carrier-phase ambiguity resolution

$$\breve{a} = \mathrm{I}(\hat{a}),\ \mathrm{I}: \mathrm{R}^n \mapsto \mathrm{Z}^n \tag{3}$$

Many such integer mappings exist. Popular choices are integer least-squares (ILS), integer bootstrapping (IB) and integer rounding (IR). ILS is optimal, as it can be shown to have the largest success rate of all integer estimators. (For further discussion of this point, see the 1999 article on the subject by P. J. G. Teunissen listed in the Additional Resources section near the end of this article.) IR and IB, however, can also perform quite well, in particular after the LAMBDA decorrelation has been applied. Their advantage over ILS is that no integer search is required.

3. Accept/Reject. Once integer estimates of the ambiguities have been computed, the third step consists of deciding whether or not to accept the integer solution. Several such tests have been proposed in the literature and are currently in use in practice. Examples include the *ratio*-test, the *F-ratio* test, the *difference*-test and the *projector*-test (See the 2005 article by S. Verhagen referenced in Additional Resources for a fuller discussion of these tests.)

The ratio-test is probably one of the most popular. If we define the (weighted) squared distance between the float solution $\hat{a}$ and an integer vector $z \in \mathrm{Z}^n$ as $D(z) = (\hat{a} - z)^T Q_{\hat{a}\hat{a}}^{-1} (\hat{a} - z)$ the ratio-test is given as

$$\text{Accept } \breve{a} \text{ if } R(\hat{a}) = \frac{D(\breve{a})}{D(\breve{a}')} \leq c \tag{4}$$

with $\breve{a}'$ being the integer vector that returns the second smallest value of $D(z)$. The positive scalar $c < 1$ is the tolerance value that needs to be selected by the user.

Thus, the decision to accept the ILS solution will be made when $D(\breve{a})$ is sufficiently smaller than $D(\breve{a}')$. Otherwise, the ILS solution is rejected in favour of the float solution.

4. Fixed Solution. Once the integer solution $\breve{a}$ has been accepted, the float estimator $\hat{b}$ is further adjusted to obtain the so-called fixed estimator

$$\breve{b} = \hat{b} - Q_{\hat{b}\hat{a}} Q_{\hat{a}\hat{a}}^{-1} (\hat{a} - \breve{a}) \tag{5}$$

This solution has a quality that is commensurate with the high precision of the phase data, provided that a correct decision was made in the preceding step. In this article, we focus attention on the third step: acceptance or rejection of the integer solution.

Although the statistical theory of integer ambiguity estimation (second step) is reasonably well established, for a long time no such theory was available for the third step. Consequently, a proper treatment of the accept/reject decision lags behind the level at which the second step is treated in practice. This has resulted in ad hoc approaches to the third step, in an absence of a proper quality description, and sometimes even in a misunderstanding of its essence.

The goal of our discussion here, therefore, is to present a unifying framework for ambiguity resolution — one that has Step 3 integrally included. The framework is based on the principle of *integer aperture estimation* as introduced by P. J. G.

Teunissen in his 2003 *Journal of Planetary Geodesy* article cited in Additional Resources.

This framework allows one to answer such questions as:
(i) What is the exact role played by Step 3?
(ii) How can we describe and evaluate its performance?
(iii) How do the different current procedures compare?
(iv) Do tests exist that are better than the current ones?

Integer Aperture Estimation

IA estimation unifies the two steps of integer estimation (Step 2) and testing (Step 3). This approach takes the float solution $\hat{a}$ as input and maps it to either an integer solution or to itself. An IA-estimator of the unknown ambiguity vector $a \in \mathbb{Z}^n$ is therefore defined as

$$\breve{a}_{\mathrm{IA}} = \begin{cases} z & \text{if } \ \hat{a} \in \Omega_z \\ \hat{a} & \text{if } \ \hat{a} \notin \Omega \end{cases} \tag{6}$$

with the subsets Ω_z, $\Omega \subset \mathbb{R}^n$ satisfying

$$\begin{aligned} &(1) \quad \Omega_z = z + \Omega_0, \ \ \forall z \in \mathbb{Z}^n \\ &(2) \quad \mathrm{Int}(\Omega_u) \bigcap \mathrm{Int}(\Omega_v) = \emptyset, \ \forall u, v \in \mathbb{Z}^n, u \neq v \\ &(3) \quad \bigcup_{z \in \mathbb{Z}^n} \Omega_z = \Omega \subset \mathbb{R}^n \end{aligned} \tag{7}$$

where Int stands for interior.

Hence, Ω is the *integer acceptance region* (fix region), while its complement is the *integer reject region* (float region). All IA-estimators have in common that their integer acceptance regions Ω are z-translational invariant, $\Omega = \Omega + z, \forall z \in \mathbb{Z}^n$. **Figure 2** shows a two-dimensional example of such a z-translational invariant acceptance region.

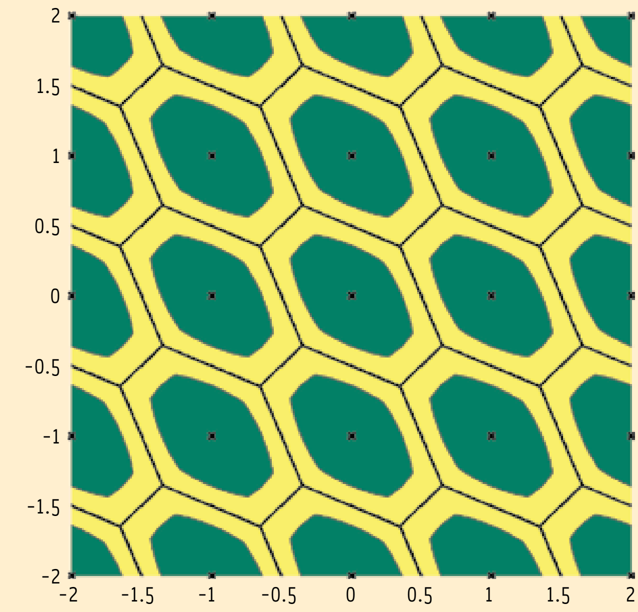

FIGURE 2 The z-translational invariant integer acceptance or fix region Ω (green area) of a two-dimensional IA-estimator

The IA-estimator is completely determined once Ω_0 is given. By changing the size and shape of Ω_0 one changes the outcome of the IA-estimator. The subset Ω_0 can therefore be seen as an *aperture pull-in region* with two limiting cases: one in which Ω_0 is empty and the other when Ω_0 is such that $\Omega = \mathbb{R}^n$.

In the first case the IA-estimator becomes identical to the float solution $\hat{a}$, and in the second case the IA-estimator becomes identical to an integer estimator. In the latter case the integer aperture pull-in regions become equal to the pull-in regions of the applied integer estimator, e.g., the ILS pull-in regions (hexagons) shown in black in Figure 2. This shows that IA-estimation generalizes the principle of integer estimation, i.e., integer estimators are IA-estimators, but the converse is not necessarily true.

Importantly, the principle of IA-estimation also generalizes all current ambiguity acceptance tests. That is, each such test procedure, such as the ratio-test, the *F*-ratio test, the difference-test, or the projector-test, is a member of the class of IA-estimators. For the ratio-test, for instance, the translational invariance of its acceptance and rejection regions follows directly from the translational invariance of $R(\hat{a})$.

This indicates that the ratio-test assesses the closeness of the float solution to its nearest integer vector. If it is close enough, the test leads to acceptance of the ILS solution; otherwise it leads to rejection in favor of the float solution. The size or aperture of the ratio-test's pull-in region provides the largest distance one is willing to accept. The tolerance value c can be used to tune this aperture.

Note that testing the closeness of the float solution to its nearest integer is not the same as testing the correctness of the ILS solution. Thus the ratio-test does not test for the correctness of the ILS solution, as is sometimes erroneously stated in the literature. The outcome of the ILS solution is correct if it would equal the unknown integer mean of $\hat{a}$, $a = E(\hat{a})$. But the closeness of $\hat{a}$ to the integer vector a is not tested by the ratio-test.

From the definition of the ratio-test, its aperture pull-in region Ω_0 can be constructed geometrically. We have

$$\begin{aligned} \Omega_0 &= \{x \in \mathbb{R}^n \mid \|x\|^2_{Q_{\hat{a}\hat{a}}} \leq c\, \|x - z\|^2_{Q_{\hat{a}\hat{a}}}, \ \forall z \in \mathbb{Z}^n\} \\ &= \{x \in \mathbb{R}^n \mid \|x + \frac{c}{1-c} z\|^2_{Q_{\hat{a}\hat{a}}} \leq \frac{c}{(1-c)^2} \|z\|^2_{Q_{\hat{a}\hat{a}}}, \ \forall z \in \mathbb{Z}^n\} \end{aligned} \tag{8}$$

where $\|.\|^2_{Q_{\hat{a}\hat{a}}} = (.)^T Q^{-1}_{\hat{a}\hat{a}}(.)$. This shows that the ratio-test's aperture pull-in region is equal to the intersection of all ellipsoids with centers

$$\frac{c}{1-c} z$$

and "radius"

$$\frac{\sqrt{c}}{(1-c)} \|z\|_{Q_{\hat{a}\hat{a}}}$$

See **Figure 3**.

Similar geometric constructions can be made of the aperture pull-in regions of the other currently used ambiguity acceptance tests, such as the *F*-ratio test, the difference-test, or the projector-test.

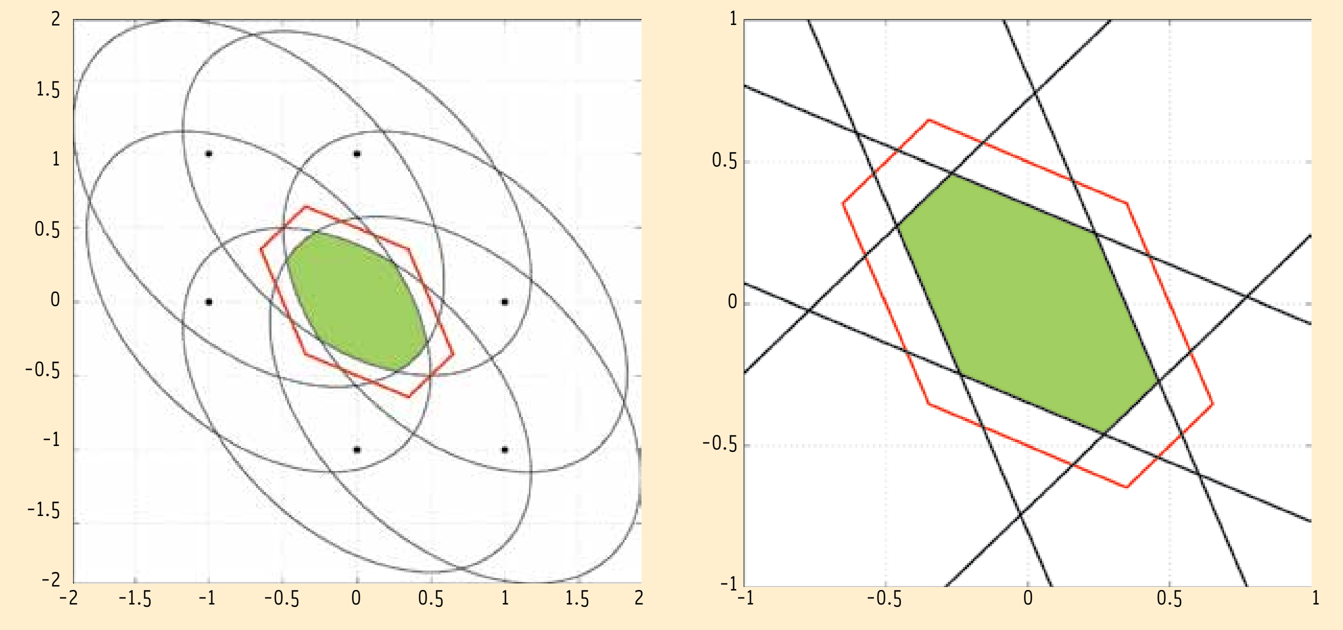

FIGURE 3 **Construction of the integer aperture pull-in regions of the ratio-test (left) and difference-test (right)**

Quality of IA-Estimation

To evaluate the performance of an IA-estimator, the following three outcomes need to be distinguished:

$$\begin{aligned} &(1)\ \breve{a}_{\mathrm{IA}} = a && \Leftrightarrow \hat{a} \in \Omega_a && \Leftrightarrow \textit{success: correct integer estimation} \\ &(2)\ \breve{a}_{\mathrm{IA}} = z \neq a && \Leftrightarrow \hat{a} \in \Omega \setminus \Omega_a && \Leftrightarrow \textit{failure: incorrect integer estimation} \\ &(3)\ \breve{a}_{\mathrm{IA}} = \hat{a} && \Leftrightarrow \hat{a} \notin \Omega && \Leftrightarrow \textit{undecided: ambiguity not fixed to integer} \end{aligned} \tag{9}$$

The corresponding probabilities of success (S), failure (F), and undecided (U) are then given as

$$\begin{aligned} P_{\mathrm{S}} &= P(\breve{a}_{\mathrm{IA}} = a) = \int_{\Omega_0} f_{\hat{e}}(x)dx \\ P_{\mathrm{F}} &= \sum_{z \in \mathbb{Z}^n \setminus \{a\}} P(\breve{a}_{\mathrm{IA}} = z) = \sum_{z \in \mathbb{Z}^n \setminus \{0\}} \int_{\Omega_z} f_{\hat{e}}(x)dx \\ P_{\mathrm{U}} &= 1 - P_{\mathrm{S}} - P_{\mathrm{F}} = 1 - \int_{\Omega_0} f_{\breve{e}}(x)dx \end{aligned} \tag{10}$$

where $f_{\hat{e}}(x)$ and $f_{\breve{e}}(x)$ are the probability density functions (PDFs) of the ambiguity residuals $\hat{e} = \hat{a} - a$ and $\breve{e} = \hat{a} - \breve{a}$, respectively. The residual vector $\hat{e}$ is the "true" ambiguity residual, while $\breve{e}$ is the estimated ambiguity residual.

Their PDFs are related as

$$f_{\breve{e}}(x) = \sum_{z \in \mathbb{Z}^n} f_{\hat{e}}(x + z)\, p_0(x) \tag{11}$$

where $p_0(x)$ is the indicator function of the ILS pull-in region of the origin. In case the float solution is normally distributed as $\hat{a} \sim N(a, Q_{\hat{a}\hat{a}})$, the PDF of $\hat{e}$ is given as

$$f_{\hat{e}}(x) \propto \exp\{-\frac{1}{2}\|x\|^2_{Q_{\hat{a}\hat{a}}}\}$$

Hence, the PDF of $\breve{e}$ is then a sum of integer-shifted normal PDFs.

For the one-dimensional case this PDF is shown in **Figure 4** for different values of $\sigma_{\hat{a}}$. A small ambiguity standard deviation $\sigma_{\hat{a}}$ tends to a Dirac impulse function, while a large $\sigma_{\hat{a}}$ tends to a uniform distribution. **Figure 4** shows examples of this point.

The above foregoing probabilities may now be used to evaluate any IA-estimator, including those that are currently in use. Additionally, these probabilities may be used to develop new strategies for current IA-estimators.

Note that the complement of the undecided probability, $1 - P_U = P_S + P_F$, is the *fix-probability,* i.e., the probability that the outcome of the IA-estimator is integer. The probability of successful fixing, the *successfix-rate*, is therefore given by the ratio

$$P_{\mathrm{SF}} = \frac{P_{\mathrm{S}}}{P_{\mathrm{S}} + P_{\mathrm{F}}} \tag{12}$$

To have confidence in the integer outcomes of IA-estimation, a user would like to have P_{SF} close to 1. This can be achieved by setting the fail-rate P_F at a small enough level.

Thus, the user chooses the small level of fail-rate that he finds acceptable and then determines the size of the aperture pull-in region Ω_0 that corresponds with this fail-rate level. With such a setting, the user has the guarantee that the fail-rate of his IA-estimator will never become unacceptably large.

This *fixed fail-rate* strategy gives users control over the fail-rate of their ambiguity resolution. And when applied to current IA-estimators, it provides an improvement over the way the tolerance values are selected.

In the case of the ratio-test, for instance, often a fixed value for the tolerance value *c* is used (e.g., ½ or ⅓). But then the user has no control over the fail-rate, because it will vary with varying strength of the underlying GNSS model. Instead of using the customary fixed *c*-value approach, the fixed fail-rate approach serves better. From the fixed fail-rate, one can then compute the variable tolerance value (which varies with the varying strength of the underlying GNSS model).

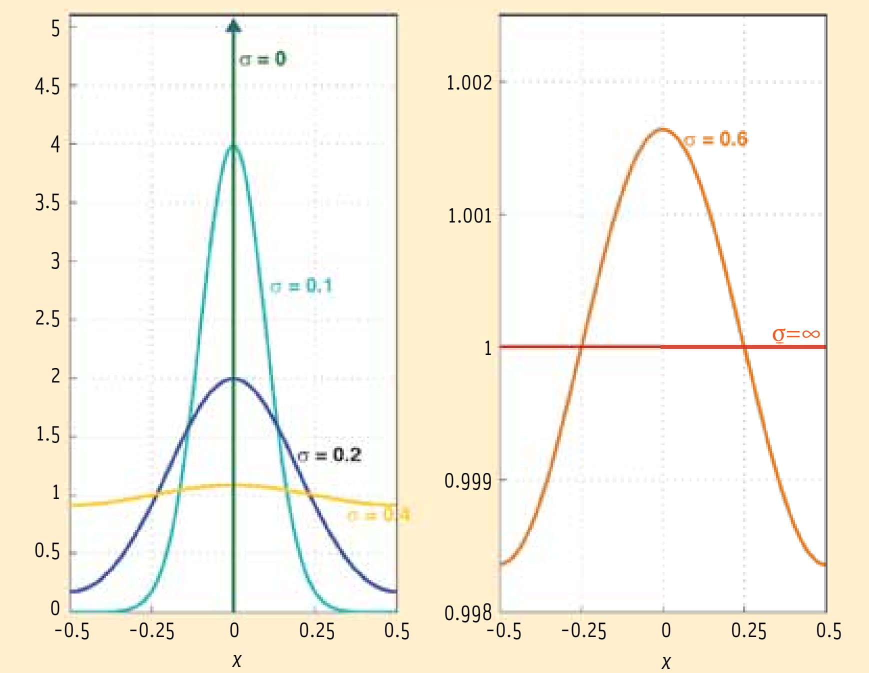

FIGURE 4 The PDF of the estimated ambiguity residual $\breve{e}$, for varying ambiguity standard deviation $\sigma_{\hat{a}}$

Optimal IA-Estimation

To this point, we have considered IA-estimation with aperture pull-in shapes chosen *a priori*, such as the ones that follow from current ambiguity tests. However, because the class of IA-estimators is much larger, one can also design one's own IA-estimator using Equation (6), simply by choosing an Ω_0 that satisfies the equations in (7). In fact, one can even go one step further and try to find an optimal IA-estimator that is best in its class.

To determine which of the IA-estimators performs best, we first need to formulate an optimality criterium. Two such optimal estimators were introduced by P. Teunissen in his 2004 and 2005 articles cited in Additional Resources. They are the *constrained maximum success-rate* (CMS) estimator and the *minimum mean penalty* (MMP) estimator.

Constrained Maximum Success-Rate (CMS) Estimator

The CMS-estimator is defined as the one that maximizes the success-rate subject to a given fail-rate. It has by definition the largest probability of correct integer estimation of all IA-estimators with the same fail-rate.

The aperture pull-in region of the CMS-estimator, $\hat{\Omega}_0$, follows from solving the constrained optimization problem

$$\max_{\Omega_0} P_S \quad \text{subject to given } P_F \tag{13}$$

The solution is given as

$$\hat{\Omega}_0 = \left\{ x \in \mathsf{P}_0 \mid \frac{f_{\hat{e}}(x)}{f_{\breve{e}}(x)} \geq \lambda \right\} \tag{14}$$

with the aperture parameter $0 < \lambda < 1$ chosen so as to satisfy the a priori fixed fail-rate P_F and where P_0 denotes the ILS pull-in region,

$$\mathsf{P}_0 = \{ x \in R^n \mid \|x\|^2_{Q_{\hat{a}\hat{a}}} \leq \|x-z\|^2_{Q_{\hat{a}\hat{a}}}, \forall z \in Z^n \}$$

This result shows that the boundaries of the optimal aperture pull-in region $\hat{\Omega}_0$ are formed by the contour surfaces of the PDF ratio $f_{\hat{e}}(x)/f_{\breve{e}}(x)$ inside the ILS pull-in region P_0. This region contracts when a smaller P_F is chosen (or λ increases). See **Figure 5** and **Figure 6** for one-dimensional and two-dimensional examples, respectively.

Figure 5 shows the PDF ratio $f_{\hat{e}}(x)/f_{\breve{e}}(x)$ in 1D for varying $\sigma_{\hat{a}}$. As the ambiguity precision improves, the aperture pull-in interval gets larger and ultimately will coincide with the interval [-0.5, +0.5].

Figure 6 shows several cases of 2D aperture pull-in regions. Those in the left plot of Figure 6 are based on a weak GNSS model (poor ambiguity precision), while those in the right plot of of the figure are based on a strong GNSS model (good ambiguity precision).

In case of the weaker model, the aperture pull-in regions are more ellipse-shaped, while in case of the stronger model the regions follow more closely the shape of the ILS pull-in region. And indeed, the stronger the model gets, the more closely $\hat{\Omega}_0$ approaches P_0.

Ultimately the CMS-estimator reduces to the ILS-estimator, $\hat{\Omega}_0 = \mathsf{P}_0$, which happens when the inequality in Equation (14) is trivially fulfilled.

Minimum Mean Penalty (MMP) Estimator

The MMP-estimator is based on the idea of penalizing certain outcomes of IA-estimation. The penalties, e.g., costs, are chosen by the user and can be made dependent on the application at hand. Different penalties are assigned to different outcomes: a success penalty p_S if $\hat{a} \in \Omega_a$, a failure penalty p_F if $\hat{a} \in \Omega \backslash \Omega_a$, and an undecided penalty p_U if $\hat{a} \notin \Omega$ ($p_S \leq p_U \leq p_F$).

With this assignment, we have constructed a discrete random variable, the penalty p, having the three possible outcomes, $p = \{p_S, p_F, p_U\}$. We may now consider the average of the discrete random variable p, the average penalty $E(p)$, which is a weighted sum of the individual penalties, with the weights being equal to the three probabilities P_S, P_F, and P_U:

$$E(p) = p_S P_S + p_F P_F + p_U P_U \tag{15}$$

The MMP-estimator is defined as the IA-estimator having the smallest mean penalty. It follows from solving the minimization problem

$$\min_{\Omega_0} E(p) \tag{16}$$

The solution is again given by Equation (14), but now with the aperture parameter given as

$$\lambda = \frac{p_F - p_U}{p_F - p_S} \tag{17}$$

Note that increasing the failure penalty, p_F, increases λ and contracts $\hat{\Omega}_0$. This is as it should be, since a contracting $\hat{\Omega}_0$ reduces the occurences of wrong fixes.

The Computational Steps

It is gratifying to see that the above two optimization principles provide the same structure for the optimal IA-estimator. It implies, somewhat in analogy with the pairing of least-squares estimation and best linear unbiased estimation, that the same procedure can be given two different interpretations of optimality.

The steps for computing the CMS- and MMP-estimator are:

- Compute the ILS-estimator

$$\breve{a} = \arg\min_{z \in Z^n} ||\hat{a} - z||^2_{Q_{\hat{a}\hat{a}}} \quad (18)$$

- Construct the ambiguity residual $\breve{e} = \hat{a} - \breve{a}$ and compute the PDF-ratio

$$\mathrm{R}(\breve{e}) = \frac{f_{\hat{e}}(\breve{e})}{f_{\breve{e}}(\breve{e})} \quad (19)$$

  This outcome provides a measure of confidence in the solution $\breve{a}$. The larger the ratio, the more confidence one has. Note that the ratio can be seen as an approximation to the successfix-rate, Equation (12). Furthermore, in a Bayesian context, $\mathrm{R}(\breve{e})$ is also the marginal posterior probability of $\breve{a}$ being the true integer vector.

- Determine the aperture parameter λ, either from the user-defined fail-rate in case of CMS, or from Equation (17) in case of MMP. Output $\breve{a}$ if

$$\mathrm{R}(\breve{e}) \geq \lambda \quad (20)$$

  otherwise the outcome is $\hat{a}$.

Both $\breve{a}$ and $\mathrm{R}(\breve{e})$ can be computed efficiently with the LAMBDA method.

Summary

IA estimation provides the framework for GNSS ambiguity resolution. It unifies integer estimation and acceptance testing in a class of ambiguity estimators for which different choices are possible. Based on the theory presented in this column, we can now answer the questions posed earlier.

1. What is the exact role played by the acceptance test (Step 3) of ambiguity resolution?

Without such testing the user would not have much control over the fail-rate. The fail-rate would then be dictated by the choice of integer estimator (e.g., ILS, IB or IR) and the strength of the underlying model. In the presence of such testing, however, the user gains control over which solutions to accept and which to reject. Hence, by exercizing control over the size of the aperture pull-in regions, the user is given control over the fail-rate of the ambiguity resolution procedure.

2. How can we describe and evaluate the performance of integer aperture estimation?

With IA estimation we can evaluate the success-, fail-, and undecided-rate, as well as the successfix-rate. This allows us then to determine an appropriate size of

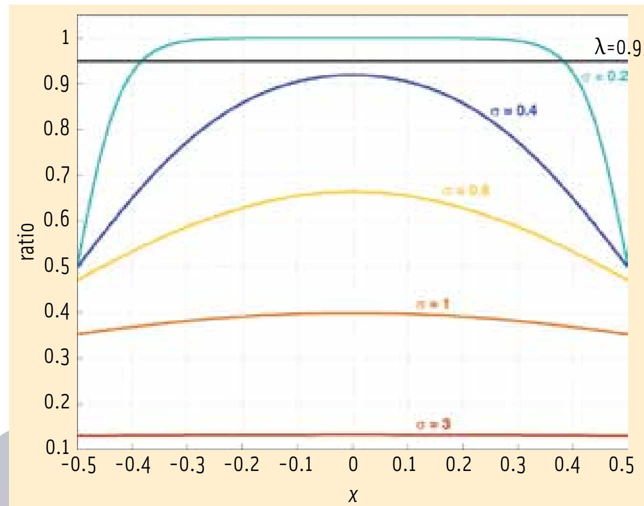

FIGURE 5 The PDF ratio $f_{\hat{e}}(x)/f_{\breve{e}}(x)$ in 1D for varying $\sigma_{\hat{a}}$

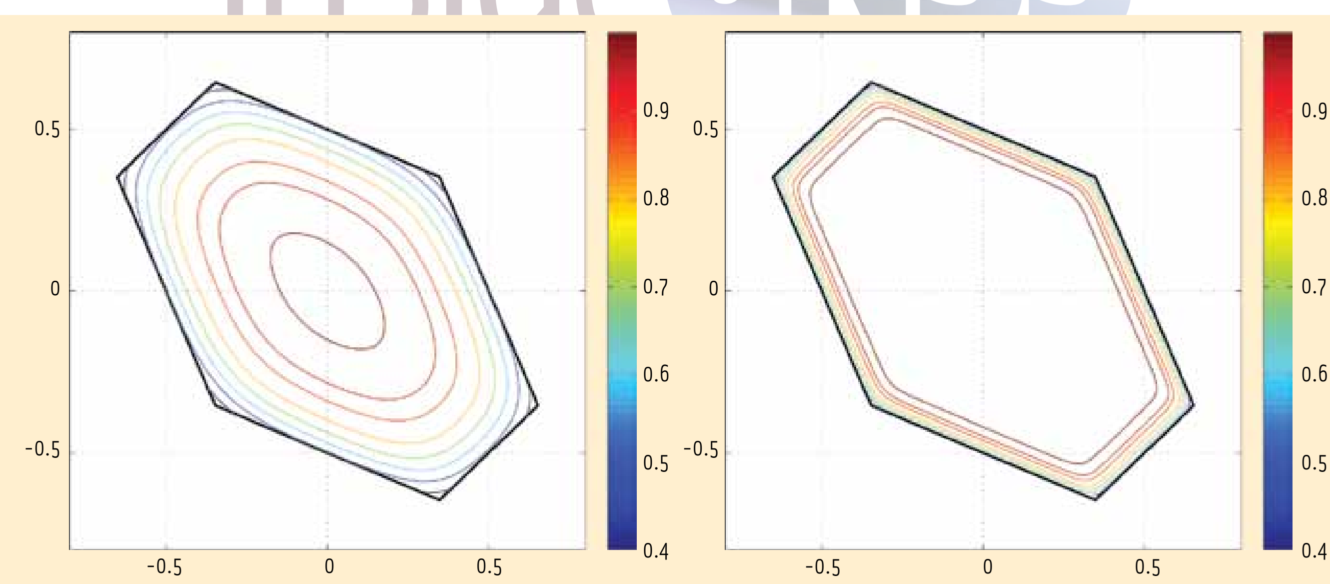

FIGURE 6 2D CMS aperture pull-in regions in case of poor (left) and good (right) ambiguity precision the aperture pull-in region, for example, by choosing a fixed fail-rate.

When a fixed fail-rate is set, the ambiguity resolution procedure automatically adapts the size of the aperture pull-in region to the strength of the underlying GNSS model. (We provide an example in the following section.) When the model gets stronger as time progresses, the size gets larger. With a sudden drop in tracked satellites, however, the size gets reduced again.

3. How do the different current procedures for acceptance testing compare?

The principle of IA-estimation provides a whole class of estimators. It can be shown that all current procedures of integer estimation and acceptance testing, such as the ratio-test, the *F*-ratio test, the difference-test, and the projector-test, are members of the IA-class. Their performance, however, will be different: the shapes of their aperture pull-in regions are different and consequently the success-rates are different too, even if the fixed fail-rate approach to select the tolerance value is applied.

4. Do tests exist that are better than the current ones?

More — and better — IA-estimators can be defined than the ones currently used. In this column, we presented two optimal integer aperture estimators: the constrained maximum success-rate estimator and the minimum mean penalty estimator. They are based on different optimality criteria but turn out to have the same structure. The difference lies in the construction of the aperture parameter.

IA Estimation Example

Figure 7 shows a two-dimensional example of IA estimation; for a given 2x2 variance matrix 10,000 float ambiguity vectors are simulated. Each dot in the figure represents a float ambiguity vector. The color depicts whether the corresponding integer solution would be accepted and correct (green), accepted and wrong (red), or rejected (blue) with IA-estimation for a certain aperture value.

In this case, the empirical fail-rate can be determined by counting the number of red dots divided by the total number of samples (10,000). The choice of a smaller aperture value will clearly result in smaller aperture pull-in regions and consequently the fail-rate will become smaller. Similarly, we can determine the empirical success-rate (by counting the green dots), which will also decrease with smaller aperture values.

For the specific example in Figure 7, the choice of the aperture value is clearly too large for the given weak model, resulting in a large fail-rate.

Figure 8 illustrates how the fixed fail-rate concept works out. Simulated float ambiguities are now shown for two different model strengths. For the weaker model (left) the spread in the float solutions is larger and consequently the aperture pull-in region should be chosen small to obtain a fail-rate of 0.1 percent in this case. For the stronger model (right), the same fail-rate is obtained with a much larger pull-in region. Hence, in this case the success- and fix-rates are also larger.

Note that the shape of the aperture pull-in regions depends on the IA-estimator and the shape of the optimal IA-estimator (CMS) is such that for a given fail-rate the corresponding success-rate is maximum.

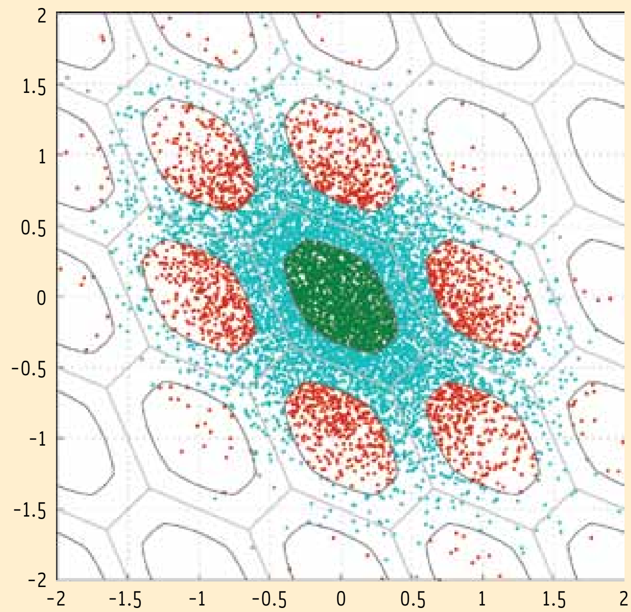

FIGURE 7 Illustration of IA estimation: simulated float ambiguities are shown as dots where the color depicts whether the corresponding integer solution would be *accepted and correct* (green), *accepted and wrong* (red), or *rejected* (blue).

Acknowledgment

Peter Teunissen is Federation Fellow of the Australian Research Council (project FF0883188). This support is gratefully acknowledged. The research of Sandra Verhagen is supported by the Dutch Technology Foundation STW, applied science division of NWO, and the Technology Program of the Ministry of Economic Affairs.

Additional Resources

[1] Abidin, H.A., "Computational and Geometrical Aspects of On-the-Fly Ambiguity Resolution," Ph.D. thesis, Department of Surveying Engineering, *Technical Report no. 104*, University of New Brunswick, Canada, 314 pp., 1993

[2] Chen, Y., "An Approach to Validate the Resolved Ambiguities in GPS Rapid Positioning," *Proceedings of the International Symposium on Kinematic Systems in Geodesy, Geomatics and Navigation,* Banff, Canada, pp. 301-304, 1997

[3] Euler, H. J., and B. Schaffrin, "On a Measure for the Discernibility between Different Ambiguity Solutions in the Static-Kinematic GPS-Mode," IAG Symposia no.107, *Kinematic Systems in Geodesy, Surveying, and Remote Sensing,* Springer-Verlag, New York City, New York, USA, pp. 285-295, 1991

[4] Frei, E., and G. Beutler.,"Rapid Static Positioning Based on the Fast Ambiguity Resolution Approach FARA: Theory and First results," *Manuscripta Geodaetica,* 15(6):325-356, 1990

[5] Han, S., "Quality Control Issues Relating to Instantaneous Ambiguity Resolution for Real-Time GPS Kinematic Positioning," *Journal of Geodesy,* 71(6):351-361, 1997

[6] Han, S., and C. Rizos, "Validation and Rejection Criteria for Integer Least-Squares Estimation," *Survey Review,* 33(260):375-382, 1996.

[7] Landau, H., and H. J Euler, "On-the-Fly Ambiguity Resolution for Precise Differential Positioning," *Proceedings of ION GPS-1992,* Albuquerque New Mexico, USA, pp. 607-613, 1992

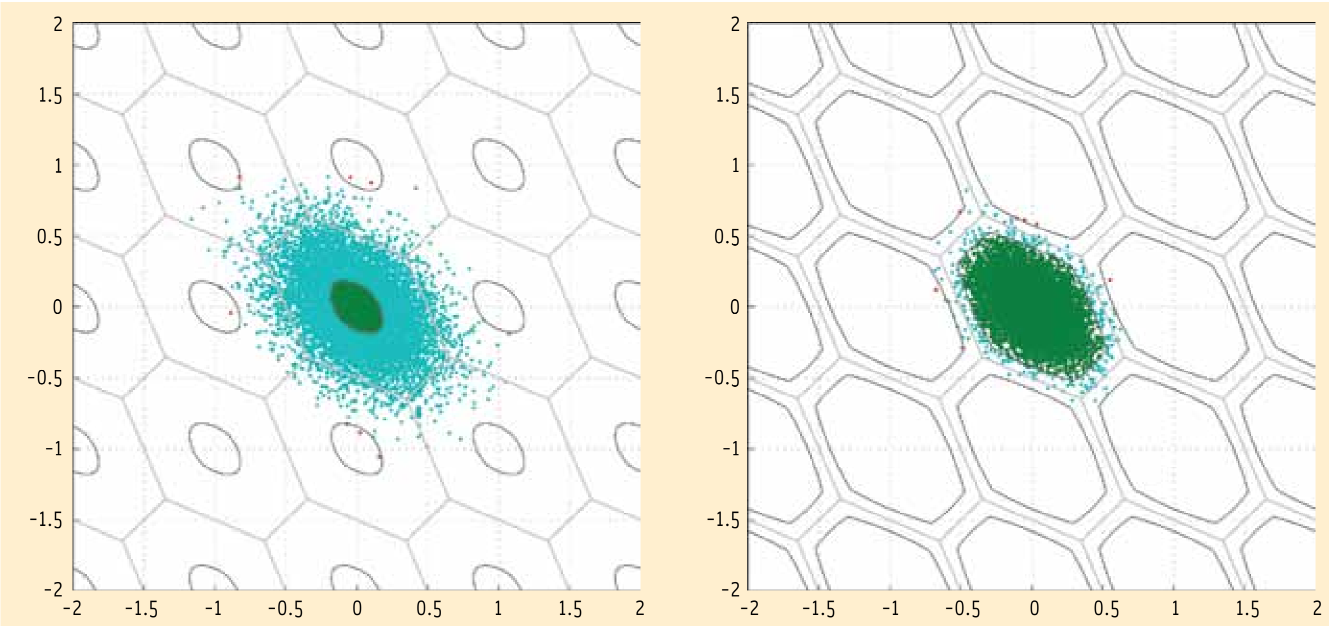

FIGURE 8 Illustration of IA estimation with fixed fail-rate for two models: simulated float ambiguities are shown as dots where the color depicts whether the corresponding integer solution would be *accepted and correct* (green), *accepted and wrong* (red), or *rejected* (blue).

[8] Odijk, D., and S. Verhagen, P. J. G. Teunissen, M. Hernandez-Pajares, J. M. Juan, J. Sanz, J. Samson, and M. Tossaint, "LAMBDA-Based Ambiguity Resolution for Next-Generation GNSS Wide-Area RTK," *Proceedings of the 2010 International Technical Meeting of The Institute of Navigation,* San Diego, California, USA, pp. 566-576, January 2010

[9] Odijk, D., and S. Verhagen, and P. J. G. Teunissen, "Medium-Distance GPS Ambiguity Resolution with Controlled Failure Rate," accepted for publication in IAG Symposia series, *Proceedings of IAG 2009,* Buenos Aires, Argentina, Springer, 2010

[10] Teunissen, P. J. G. (1999), "An Optimality Property of the Integer Least-Squares Estimator," *Journal of Geodesy,* 73(11):587-593, 1999

[11] Teunissen, P. J. G. (2002), "The Parameter Distributions of the Integer GPS Model," *Journal of Geodesy,* 76(1):41-48, 2002

[12] Teunissen, P. J. G. (2003), "Integer Aperture GNSS Ambiguity Resolution," *Artificial Satellites, Journal of Planetary Geodesy,* 38(3):79-88, 2003

[13] Teunissen, P. J. G. (2004), "Penalized GNSS Ambiguity Resolution," *Journal of Geodesy,* 78(4-5):235-244, 2004

[14] Teunissen, P. J. G. (2005), "GNSS Ambiguity Resolution With Optimally Controlled Failure-Rate," *Artificial Satellites,* 40(4):219-227, 2005

[15] Teunissen, P. J. G. (2010), "Mixed Integer Estimation and Validation for Next Generation GNSS," in: *Handbook of Geomathematics, Ch. 37,* W. Freeden, M. Nashed, T. Sonar (Eds), 2:1101-1128, 2010

[16] Teunissen, P. J. G., and S. Verhagen, "The GNSS Ambiguity Ratio-Test Revisited: A Better Way of Using It," *Survey Review,* 41:138-151, 2009

[17] Tiberius, C. C. J. M., and P. J. De Jonge, "Fast Positioning Using the LAMBDA Method," in *Proceedings of DSNS'95,* Bergen, Norway, paper no. 30. The Nordic Institute of Navigation, Oslo, 1995

[18] Verhagen, S. (2005), "The GNSS Integer Ambiguities: Estimation and Validation," Ph.D. thesis, *Publications on Geodesy,* 58, Netherlands Geodetic Commission, Delft, 2005

[19] Verhagen, S., (2006), "Improved Performance of Multi-Carrier Ambiguity Resolution Based on the LAMBDA Method," *Proceedings of Navitec 2006, ESA/ESTEC,* Noordwijk, The Netherlands, 2006

[20] Verhagen, S., and P. J. G. Teunissen, "New Global Navigation Satellite System Ambiguity Resolution Method Compared to Existing Approaches" *Journal of Guidance, Control, and Dynamics,* 29(4):981--991, 2006.

[21] Verhagen, S., and P. J. G. Teunissen, "On the Probability Density Function of the Ambiguity Residuals," *GPS Solutions,* 10:21-28, 2006

[22] Wang, J., M. P. Stewart, and M. Tsakiri, "A Discrimination Test Procedure for Ambiguity Resolution on-the-Fly," *Journal of Geodesy,* 72(11):644-653, 1998

Authors

Peter J. G. Teunissen is a professor of geodesy and Earth observation, Federation Fellow of the Australian Research Council (ARC), and Positioning Science Director of the Cooperative Research Centre for Spatial Information (CRC-SI). His current research focus is on modeling next-generation GNSS for high-accuracy relative navigation and attitude determination in space and air. He is the inventor of the LAMBDA method and has more than 25 years of GNSS research experience.

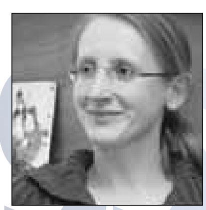

Sandra Verhagen obtained her Ph.D. from Delft University of Technology (DUT) and is now an assistant professor at DUT. Her research focuses on ambiguity resolution and integrity monitoring for real-time kinematic GNSS applications, for which she received a research grant from the Dutch Science Organisation (NWO). She is president of commission 4 Positioning and Applications of the International Association of Geodesy (IAG).

Guenter W. Hein serves as the editor of the Working Papers column. He is head of the Galileo Operations and Evolution Department of the European Space Agency. Previously, he was a full professor and director of the Institute of Geodesy and Navigation at the University FAF Munich. In 2002 he received the prestigious Johannes Kepler Award from the U.S. Institute of Navigation (ION) for "sustained and significant contributions to satellite navigation." He is one of the CBOC inventors. IG